Dynamics of developable cones under shear

Eugenio Hamm,* Benoît Roman,† and Francisco Melo
Departamento de Física de la Universidad de Santiago de Chile, Avenida Ecuador 3493, Casilla 307 Correo 2, Santiago, Chile and Center for Advanced Interdisciplinary Research in Materials (CIMAT), Avenida Blanco Encalada 2008, Piso Zócalo, Santiago, Chile

(Received 6 December 2003; published 26 August 2004)

We identify and study a persistent structure characteristic of the post-buckling regime of a thin cylindrical shell subjected to axial torsion. It consists of a pair of developable cones (*d* cones) joined by an S-shaped ridge, having a size of the order of the radius of the cylinder. We study its formation by applying a concentrated load at the center of the shell, which creates an isolated pair of *d* cones, joined by a straight ridge that progressively tilts when a torsion angle is imposed. We interpret this response as the equilibrium state of a pair of interacting *d* cones in the presence of an in-plane shear field, created by axial torsion, which tends to drive them away from each other. We find that the amplitude of displacement of the *d* cones for a given torsion angle is amplified by decreasing the thickness of the sheet, therefore concluding that the equilibrium state is the result of a balance between bending and stretching energies. We propose a model where the driving effect is the coupling between the deformation field around the *d* cones and the imposed shear field, while the stabilizing effect is the increasing bending energy of the system.

DOI: 10.1103/PhysRevE.70.026607 PACS number(s): 46.25.Cc, 46.70.−p, 46.90.+s

I. INTRODUCTION

The deformation of elastic thin-walled objects like plates and shells, subjected to load, have received much attention in the last century mainly in the context of structural design [1,2]. Particularly the buckling of thin-walled objects is a matter of considerable effort. Although the threshold and buckling modes are now well documented for simple geometries, the post-buckling behavior arising for high strains remains largely unknown. Only recently have some answers to these questions been given in terms of robust line and point defects—respectively, ridges [3–5] and developable cones (*d* cones) [6–8], which play a central role in the process of the folding and crumpling of thin sheets [9]. When a sheet of paper is crumpled and unfolded back, the structure of irreversible deformation consists of a network of ridges joined at *d* cones. In the framework of nanostructures, the bending and ripple formation in carbon nanotubes has been described as well [10]. The dynamics of *d*-cone defects is the subject of growing interest. For instance, a plate that is bent along one direction into an arch and then forced to bend in the perpendicular direction by applying a concentrated load at its surface exhibits a defect-mediated transition to uniform buckling, in which *d*-cone singularities follow complex motions as the load is increased [11].

Here we study experimentally the motion undergone by *d*-cone singularities in thin sheets, when subjected to in-plane shear. This situation arises generically when a thin-walled cylinder is twisted far above its buckling threshold. In order to nucleate *d* cones we impose a radial displacement concentrated in one point on the surface of a cylindrical shell. For this geometry, inspired by [11], *d* cones are always nucleated pairwise. By increasing the radial displacement the *d* cones move apart perpendicularly to the cylinder's axis as a climbing mode in analogy to defect motion in crystals. In contrast, when the cylinder is twisted around its axis we observe that *d* cones move parallel to the axis of the cylinder in a gliding mode. Therefore the *d* cones show a robust dynamical behavior consisting of two pure modes of motion which can be clearly distinguished separately. This is analogous to the behavior of an edge dislocation in a crystal subjected to an external stress field, in which case the Burgers vector is a measure of the size of the defect and determines its dynamics under external fields. Here we show that the amplitude of gliding motion is not simply a geometrical effect but instead appears to be thickness dependent and, therefore, is a result from a balance between bending and stretching energies.

The article is structured as follows. We start in Sec. II by describing the experimental setup and methods. Then, in Sec. III we describe an experiment characterizing qualitatively the successive stages of buckling of the cylindrical shell subjected to increasing torsion, up to its complete crumpling, and show that they all include a robust S-shaped structure that we study in the rest of the paper. The main part of this work is found in Sec. IV, where we describe an experiment which allows us to isolate a single S-shaped structure by imposing a radial displacement concentrated in one point on the surface of the shell and study the displacement of the *d* cones when torsion is applied. We report measurements of amplitude of the gliding mode of *d* cones for increasing values of the radial displacement and twisting angle. We also show measurements of the force and torque corresponding to these degrees of freedom. Finally, in Sec. V we propose a

*Electronic address: lhamm@usach.cl
†Present address: PMMH-ESPCI-10 rue Vauquelin, 75231 Paris Cedex 5, France.

 ©2004 The American Physical Society

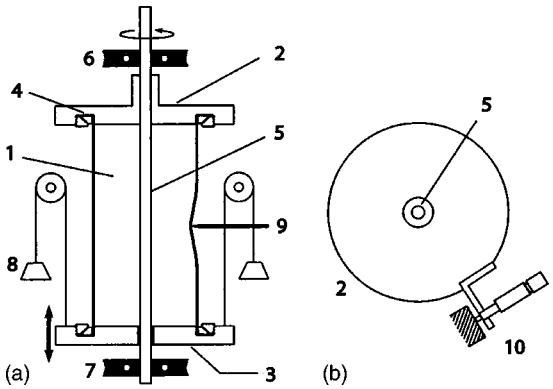

FIG. 1. Side (a) and up (b) views of the experimental setup. (1) Cylindrical shell. (2) Upper disk (rotation only). (3) Lower disk (vertical translation only). (4) Attachment system for clamped boundary conditions. (5) Axis. (6) Upper bearing. (7) Lower bearing. (8) Counterbalance. (9) Finger for concentrated radial displacement. (10) Micrometer screw to apply rotation to upper disk. The upper disk is fixed to the axis while the lower is not. The system that prevents the lower disk from rotating is not represented.

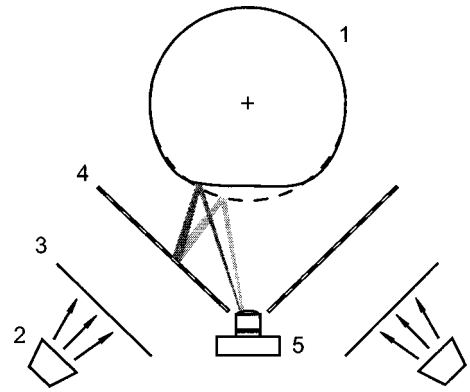

FIG. 2. Setup for visualization of deformation by measurement of the local tangent angle of the deformed cylinder. (1) Cylindrical shell (solid line, deformed cylinder: dashed line, nondeformed). (2) Light sources. (3) Light diffusers. (4) Panels with stripe pattern. (5) Camera/video.

phenomenological model that captures the main features of the experimental observations.

II. EXPERIMENTAL SETUP

The cylindrical shell is obtained from a flat, reflecting, PVC sheet that is bent and joined at the meeting edges and clamped at its ends. It has a height $L=43.5$ cm and an internal radius $R=6$ cm. The sheet thickness varies from $h=0.1$ to 0.5 mm, which are appropriate for the stiffness of the setup. Each end of the cylindrical shell is fixed by fitting it around short rigid cylinders and clamped from outside by a wedged plastic ring which is sandwiched between the sheet and another wedged circular metallic ring which compresses the plastic ring by screwing it [Fig. 1(a)]. This provides a uniform clamping for the sheet.

The difficulty to obtain a perfectly cylindrical shell was overcome by means of a very refined bond method. The originally flat sheet is cut at a slightly greater length than the required perimeter. The joining sides of the sheet are then scraped in such a way that they can be bonded without augmenting the local thickness of the sheet. Without this caution the fixed edge boundary conditions would be severely affected as the compression produced by the outer ring would not be uniform. To get the desired radius, the sheet is coiled around an auxiliary solid cylinder with the same radius $R=6$ cm, which is removed after the sheet is glued. The setup allows the evacuation of air when the cylinder starts to buckle and the volume enclosed by it diminishes.

The top side of the cylinder can be forced into torsion by rotation of the upper disk thanks to a micrometer screw [Fig. 1(b)]. For extremely large rotation this system is replaced by a stepping motor. The rotation of the lower disk is prevented by two vertical cylindrical bars, which can only glide vertically through ball bearings. This setup imposes on the cylinder a constant vertical force that can be adjusted through the choice of a counterweight. In this experiment we chose to fix it to zero.

In order to create an isolated pair of *d* cones we place in the middle region of the cylinder a rounded solid finger that can be moved radially towards the cylinder [Fig. 1(a)]. When the finger pushes down the surface of the cylinder, a pair of *d* cones nucleates symmetrically around the finger. By then twisting the cylinder around its axis, the positions of the *d* cones are modified by the induced in-plane shear. Visualization of the deformation experienced by the cylindrical shell is accomplished by the following procedure. We place, symmetrically in front of the observation region, two panels with a regular pattern of vertical black lines on bright background. Pictures are taken of the reflection of the lines on the surface of the cylinder. When the shape of the surface of the cylinder changes, the reflected pattern of lines deforms (Fig. 2). Typi-

FIG. 3. Initial buckling pattern on the cylinder under torsion

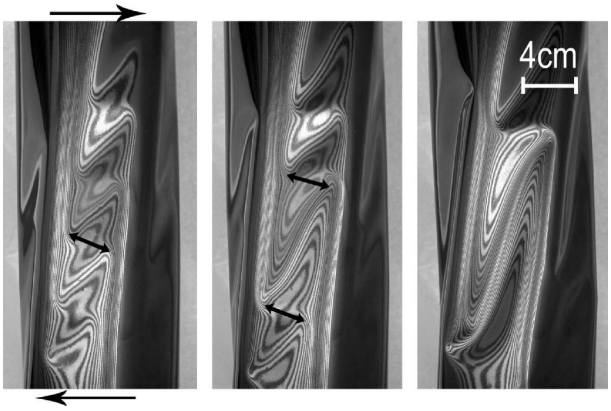

FIG. 4. Three stages of annihilation of *d* cones and merging of ridges for increasing torsion. The arrows represent the sense of shear induced by torsion. Double arrows indicate the pair of *d* cones that annihilate at the next stage. Note that two annihilating *d* cones are rotated in π, one relative to the other.

cal pictures obtained by this method are presented in Figs. 3–6.

III. PURE TORSION OF A CYLINDRICAL SHELL

A. Typical experiment overview

A thin cylindrical shell of elastic material buckles when it is subject to torsion around its axis. The linear theory for not too long cylinders [1,2] predicts a critical torsion angle and a critical torque at which the cylinder buckles with a characteristic helicoidal pattern having an integer number of azimuthal wavelengths, superimposed with an integer number of longitudinal wavelengths and a pitch of the helix (Fig. 3). The validity of a linear theory is given by the dimensionless parameter L^2/Rh, where L, R, and h are, respectively, the length, the radius, and the thickness of the cylindrical shell. In the range 20–1000 it shows reasonable agreement with experiments. Beyond this range all linear theories fail and only qualitative conclusions can be drawn. In our experiment this quantity is of the order 10 000, excluding any quantitative matching with the available theory. By applying axial torsion to a long cylindrical shell of thickness $h=0.2$ mm, we obtained the aforementioned helicoidal pattern (Fig. 3). This deformation is accompanied by a smooth elastic energy distribution. When the torsion angle is increased, the deformation of the shell is accompanied by focusing of the energy along narrow straight regions called ridges [3–5], which are articulated around pointlike regions called *d* cones [6–8]. For increasing torsion, the *d* cones start to collapse pairwise with a characteristic pop noise. This process is such that two vertical wavelengths merge into one, leaving the number of circumferential wavelengths unchanged (Fig. 4). By means of this inverse cascade process the number of longitudinal waves decreases progressively, one at a time. After having attained a certain torsion angle all *d* cones have mutually annihilated, leaving only one longitudinal wavelength, approximately at the center of the cylinder (Fig. 5). Outside this region the cylindrical shape of the shell has been restored, indicating that the in-plane shear stress has dropped below the buckling critical stress. This behavior is similar to the one observed in a long cylinder subject to axial compression, where deformation also localizes around its central part and the buckling critical stress is well below the predicted

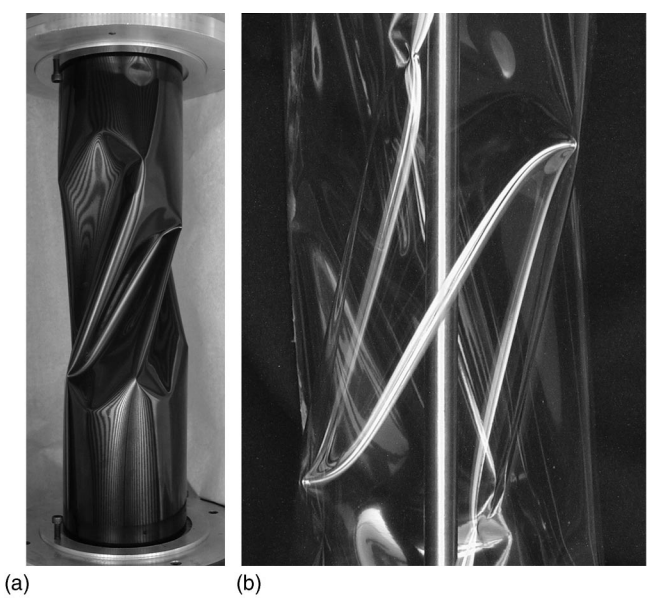

FIG. 5. Localized azimuthal pattern and typical S structure. (a) Nontransparent cylindrical shell with $L=44.5$ cm, $R=6$ cm, and $h=0.20$ mm. (b) Closer view of an S structure in a transparent shell, obtained by simple reflection of a light source, having the same dimensions as (a). Note that the axis of the setup is visible.

FIG. 6. Secondary S structure after locking of the primary pattern. There is a hierarchical cascade of S-structure formation for increasing torsion.

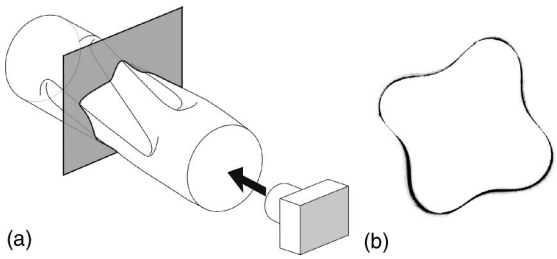

FIG. 7. (a) Experimental setup for the laser-sheet technique. (b) Typical picture obtained by this method, allowing the reconstruction of the surface of the cylinder.

values given by linear theories [12]. The remaining *d* cones can no longer annihilate and, as the torsion angle increases further, they become more pronounced leading to plastic deformations.

Ultimately the cylinder folds along the ridges obstructing itself or touching the axis of the setup. The buckling then reinitiates in the remaining smooth parts of the shell, with the central region acting as an effective boundary (Fig. 6). This is the beginning of a buckling and folding cascade which continues until the whole shell has folded.

At all described stages we observe a characteristic shape given by a pair of *d* cones joined by an S-shaped ridge (Fig. 5). The small deviations from a straight line, particularly near the core of the *d* cones, indicate the presence of in-plane stretching. We call the whole structure the S structure.

This overview shows a very rich behavior when the cylindrical shell is forced into torsion. At every stage of deformation beyond the buckling threshold, as soon as strain becomes large, the S structure is the fundamental equilibrium shape. We focus now in the characterization of this structure.

B. Tridimensional shape

In this section we characterize the tridimensional S structure using a laser-sheet technique. A He-Ne laser plane, perpendicular to the axis of the cylinder, illuminates the points in the shell that are intersected by the plane of the laser and a picture is taken in the direction of the axis. This technique required the design of special transparent disks for the fixed boundary conditions at the extremes of the cylinder [Fig. 7(a)]. A typical image obtained in this way is shown in Fig. 7(b). Computer treatment of these images taken for various positions of the laser plane detects the position of the section and allows reconstruction of the whole three-dimensional surface [Fig. 8(a)]. Figure 8(b) represents one S structure taken from three different views. The two lateral views show that the line joining the points of minimum distance to the axis is mostly straight, so that the S-shaped ridge is also mostly included in a plane parallel to the axis. In contrast, the frontal view indicates nondevelopable regions near the core of the *d* cones, which are possible only via in-plane stretching deformations. See also Fig. 5.

For thin shells, the energy required for stretching is very large compared to that for bending [13], so that deformations isometric to the plane are preferred. The only possible smooth deformations of this kind are those leading to conical

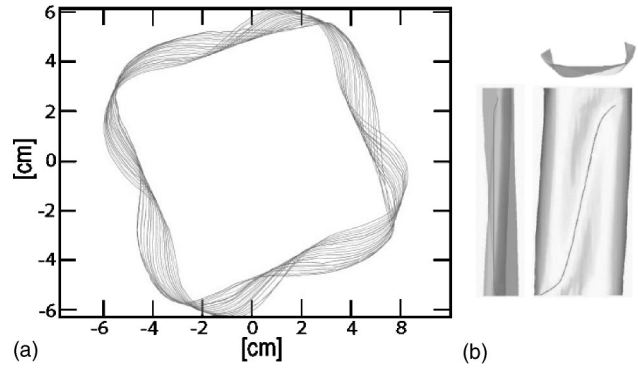

FIG. 8. (a) Superposition of successive laser planes in the central region of the cylinder. (b) Top, lateral, and front views of the reconstructed S structure. The lines connect the minimum local distances measured from the surface to the axis.

or cylindrical surfaces. However, when externally imposed restrictions are severe, a situation like this may be impossible without in-plane stretching. In order to minimize energy, the regions where stretching is important become very narrow (stretching ridges) or localized (*d* cones). In the cores of these defects, stretching and bending energies are of the same order, this balance determining the sizes of the respective cores. Outside these regions the shell is developable—i.e., has zero Gaussian curvature.

At early stages of buckling the energy distribution is rather smooth. Thus, the condition for focusing of energy necessary for *d*-cone and ridge nucleation can be fulfilled more easily in a post-buckling regime, where for increasingly large torsion the sheet gradually folds. In this stage the regions near the core of *d* cones become clearly nondevelopable (Fig. 5) while the ridges become more pronounced and do not change their length significantly. Rather they tilt progressively until they attain a nearly horizontal orientation. In this process the *d* cones act as hinges that articulate the ridges. In addition, the only region where permanent plastic deformation is visible corresponds to the core of the *d* cones. This interpretation is enforced by the experimental observation that in the post-buckling regime the torque weakly increases for increasing torsion, indicating that in-plane shear stress is not varying significantly. Note that in regions where no buckling has occurred, the in-plane shear stress stays relatively constant while most of the deformation is absorbed in the S structures. At this point an important difference between the well-known *stretching ridge* and the S structure reported here comes to mind; an S structure can be seen as a laterally curved ridge in which most of the stretching is due to this additional curvature located near the *d* cones.

IV. ISOLATED S STRUCTURE

We focus now on the S structure, isolated by the method described in Sec. II, which allows the nucleation of a pair of *d* cones symmetrically around the finger in such a way that the ridge joining them is perpendicular to the axis of the cylinder [Fig. 9(b)]. Our setup is similar to that of [11], the difference being that in our case the cylinder is closed and

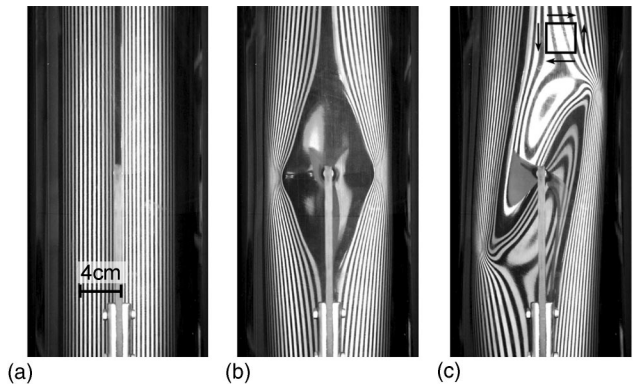

FIG. 9. Deformation of a cylindrical shell of thickness 0.2 mm, for different values of z and θ. (a) Nondeformed cylinder, $z=0$, $\theta=0$. (b) $z=10.1$ mm, $\theta=0$. (c) $z=10.1$ mm, $\theta=0.026$ rad.

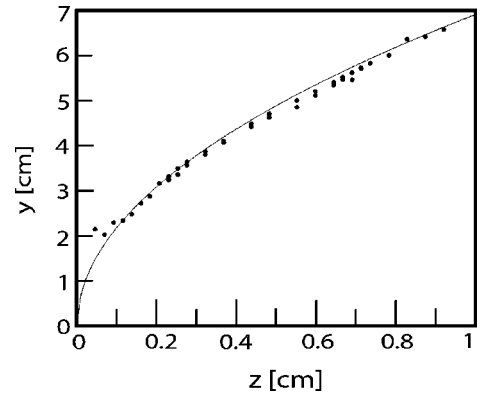

FIG. 10. Lateral position y as a function of z without torsion for a sheet of thickness 0.2 mm. The solid line is the geometric model's prediction.

fixed at its ends. When axial torsion is imposed the d cones move to a new position [Fig. 9(c)]. The position of the finger, z, measured inwards from the surface of the nondeformed cylinder, and the angle of rotation, θ, imposed on the upper end of the cylinder, are the two main control parameters. The highest value of θ is determined by the onset of buckling. For large z the buckling transition is retarded. Therefore to increase the range of experimental data we prefer to fix a distance z and then apply a rotation angle θ. When z is comparable to the sheet thickness [11] we can observe two d cones, whose positions are a function of z and θ. We measure the vector that joins them and denote (x,y) its coordinates in a plane perpendicular to the pushing finger. By definition this plane contains the S structure. Coordinate x is parallel to the cylinder's axis and y perpendicular.

We note that by adding a second finger it is possible to study the mutual annihilation of d cones. By pushing the two fingers or by twisting the cylinder, two S structures are forced to approach mutually and eventually merge into one S structure by annihilation of a pair of d cones (see Sec. III A and Fig. 4).

A. Kinematics of *d* cones

1. Detection of singularities

In order to track the positions of the d cones we use the same visualization method described in Sec. II, for a sheet of thickness $h=0.2$ mm. The position along the axis or vertical position of the singularities is easy to determine as it is the place of maximum lateral deflection of the lines. The lateral position y is less easy to measure as it requires a criterium for the definition of the center of the d cone. The d cone is not symmetric in the y direction. A computer code computes, according to geometrical optics, the angle of the tangent plane to the surface. This is possible with a precise knowledge of the position of each black line on the initial pattern with respect to the camera and to the cylinder. Knowledge of the angle gives then a measure of the horizontal curvature by differentiation, and the singularity is then located at the point where curvature is a maximum. As the same image obtained by reflection can be obtained from a variety of different deformations, the inward deformation of the surface in the computation for the angle of reflection is assumed to be close to that imposed by the finger.

2. Climbing mode at $\theta=0$

By imposing a radial displacement of the finger without applied torsion [Fig. 9(b)], the d cones move in a climbing mode at $x=0$. The position of the d cones, as a function of the imposed radial distance z, is represented in Fig. 10 and follows very well the law $y=2\sqrt{2Rz}$ [11]. This comes from the simple fact that both d cones are joined by an inward ridge which is essentially straight and has a depth z at its center, measured from the originally cylindrical surface. A first approximation is that the d cones are at the intersection of the line along ridge with the originally nondeformed cylindrical surface. We checked this law for our setup obtaining good agreement.

We found also that this result extends when torsion is applied since the singularities move mainly in a direction along the axis of the cylinder while the displacement in the perpendicular direction is negligible [Fig. 9(c)]. This is explained by the fact that the picture of the intersection of a line with the cylinder remains unchanged if we consider the projection of the line onto the (y,z) plane. Note that the lateral position y of the singularities can thus be deduced by geometrical arguments, independent on the thickness of the sheet.

3. Gliding mode under applied torsion

When torsion is imposed, we observe that the d cones move mainly parallel to the axis to a new position, but in opposite directions; this asymmetry leading to the formation of the S structure [Fig. 9(c)]. Figure 11 represents the dependence of y on increasing z for different values of θ. The broadening of the curve shows a weak growing dependence of y on increasing θ at fixed z, which is much smaller than the variation experienced by x for the same θ. In fact, the effect of torsion can be very impressive on x, creating large S structures for high values of z. As seen in Fig. 12, x grows linearly with θ, the coefficient of proportionality being a

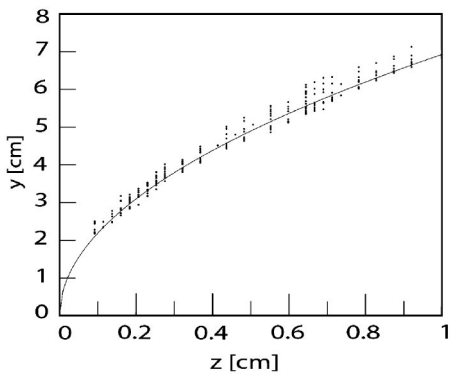

FIG. 11. Position of the singularities in the y direction as z is increased, for different values of θ.

growing function of z. If now x is plotted against z (Fig. 13) for several values of θ, we obtain also a linear dependence and identify, for $h=0.2$ mm, a threshold value, $z_0 \approx 1.4$ mm, which separates two regimes. The first one, valid for $z < z_0$, shows that d-cone displacement is not sensitive to torsion, whereas for $z > z_0$ it has a finite effect. In contrast, the onset of displacement reveals no threshold value for the angle of rotation. Figure 14 shows a collapse of all the experimental points on a single line, suggesting that x goes linearly with $\theta(z-z_0)$, with a very large nondimensional coefficient.

B. Dynamics of *d* cones

To better understand the origin of the aforementioned large coefficient we repeated the experiment using sheets having different thicknesses. The results for four thicknesses are shown in Fig. 15, where a normalization in h^{-1} produces a collapse of all the curves. We note also that there is a variation in z_0 which shows a growing dependence with h. The best fit of the data gives

$$\frac{x}{R} = \alpha \frac{z - z_0}{h} \frac{R\theta}{L}, \tag{1}$$

where $\alpha \approx 24$. This behavior is valid until the onset of buckling, which corresponds to a displacement x saturating at values of the order of the radius R of the cylinder.

The fact that x is dependent on thickness through Eq. (1) shows clear evidence that the displacement of d cones in the presence of a shear field is not a purely geometrical effect but involves simultaneous bending and stretching deformations. By "purely geometric" we mean a situation in which the equilibrium state is controlled only by bending deformations that minimize the energy. The sheet avoids any stretching deformation by keeping the surface isometric to the plane so that the equilibrium shape of the sheet can be predicted by geometrical arguments which are independent of thickness.

An interesting application for Eq. (1) is that it constitutes a very sensitive test to detect residual shear stress in a thin sheet because of the large factor involving the inverse of the thickness of the sheet. It suffices to bend the sheet as a cylinder and to push it radially at a point: if the ridge joining the two resulting d cones is not perpendicular to the axis of the cylinder, then there is some residual stress present.

We have measured both the lateral force at the finger and the torque necessary to twist the cylinder by means of strain gauges. The applied force F_z for $\theta=0$ is shown in Fig. 16 for three different thicknesses of the sheet, with a collapse on a master curve in the plane $[FR/Yh^3, z/h]$. The scalings allow us to identify three regimes. The first, valid for $z \ll h$, predicts a linear response of the force with z [13], such that $F_z R/Yh^3 \sim z/h$. In this regime the resulting deformation is localized in a region of size $\sim\sqrt{Rh}$ and arises from a balance between bending and stretching energies. In a second regime, valid for $z \sim h$, the deformation energy comes mainly from

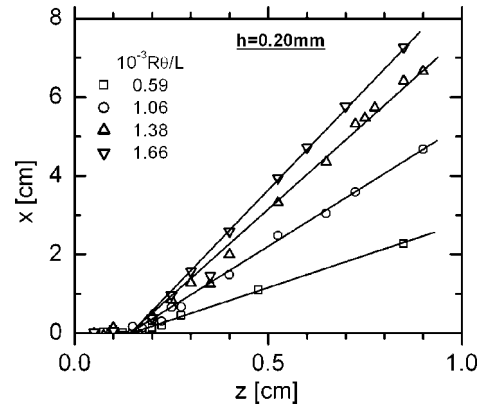

FIG. 13. Vertical position x of the pair of d cones, as a function of z for different values of θ.

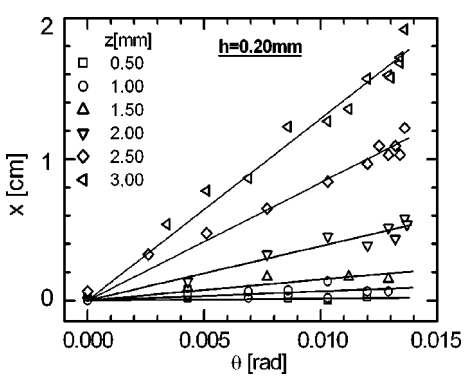

FIG. 12. Vertical position x of the pair of d cones, as a function of θ for different values of z.

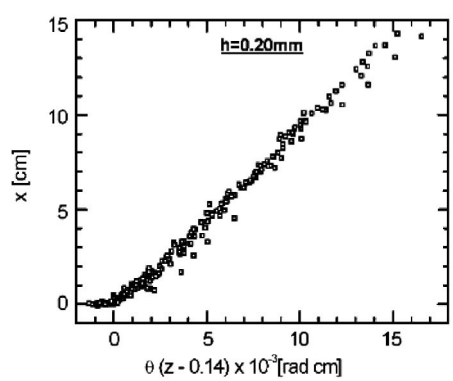

FIG. 14. Vertical position x of the pair of d cones, as a function of $\theta(z-z_0)$.

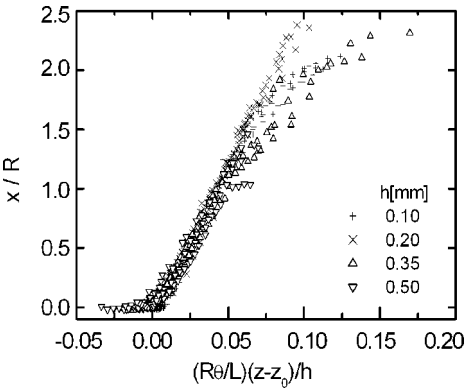

FIG. 15. Vertical position of the d cones for different thicknesses h of the sheet. The constant z_0 is a function of h.

the pair of nucleated d cones in the form of bending [11]. The force and bending energy show both a logarithmic dependence in z/h, which is related to the finite size of the core of the defect, and a coefficient containing a geometric factor [8,11]. The contribution of the cores to the total energy is negligible. Beyond a crossover region situated around $z \sim 5h$ we find a third regime characterized by a deviation from the logarithmic behavior and a slight splitting of the curves, indicating that the deformation is not due solely to the two d cones. In fact, the restriction imposed by the finger is severe in the sense that the sheet has to accommodate three developable surfaces—namely, both d cones and the original cylindrical surface. This cannot be accomplished without stretching deformations necessary to join distinct locally developable surfaces. In this regime the sheet selects a deformation minimizing its total elastic energy and therefore the force v/s displacement relation is different for different thickness. We note from Fig. 16 that, for $z \gtrsim h$, F_z scales roughly linearly with z and is proportional to h^2.

The experimentally found threshold value z_0 for d-cones displacement is compatible with the existence of the crossover region centered at $z \sim z_0 \sim 5h$ in Fig. 6. Beyond z_0 the sheet has an equilibrium state that combines in-plane stretching and bending deformations that minimize the elastic energy; the dependence of the force on h^2 is the natural consequence of this fact. Below z_0, the force on the tip is compatible with d cones where bending is the dominant contribution to the energy.

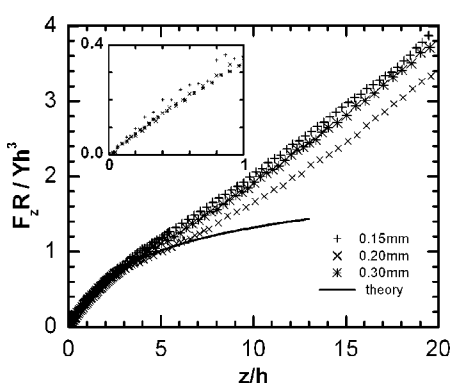

FIG. 16. Lateral force v/s z at the finger for $\theta=0$ for three different thicknesses of the PVC sheet. Inset: for $z \ll h$ the force goes linearly with z. The solid line corresponds to the model proposed in [11] for values of z of the order of h. The best fit gives $F_z R/Yh^3 = 0.44 \ln(2.01 z/h)$.

V. ANALYSIS AND DISCUSSION

We now discuss our main experimental result concerning the displacement of the d cones under imposed shear, condensed in the very simple scaling law (1). We interpret this in terms of a particle+field description such that each d cone is a particle immersed in the shear field arising from torsion of the cylinder. The applied shear field produces a force on the d cone that drives it to a new position where it is balanced by an opposite force derived from an increasing bending energy. This dynamics is best described by looking at the energies involved, which we develop at lowest order in x.

We first evaluate the variation in bending energy due to a displacement x of the d cones. Following [8], the bending energy of a generic d cone in a circular domain of radius R is given by $E_b = C_0 Y h^3 \epsilon^2 \ln(R/R_c)$, where C_0 depends on the Poisson ratio σ of the material and contains a geometric factor, ϵ is the amplitude of the d cone, and R_c is a cutoff radius. We generalize this result to the case when the domain where deformation arises is not circular. The energy is then

$$E_b = \frac{Yh^3}{24(1-\sigma^2)} \epsilon^2 \int_{-\pi}^{\pi} f(\theta) \ln\left(\frac{R(\theta)}{R_c}\right) d\theta. \tag{2}$$

Here, $f(\theta)$ is proportional to the square of the local curvature of the sheet and $R(\theta)$ is the angle-dependent radius of integration. Consider the reference state given by a pair of d cones at $x=0$. Let $E_b^{(0)}$ be the energy of this configuration and let $R_0(\theta)$ be the radius of integration, which is of the order of the middistance between the two d cones, $y/2 = \sqrt{2Rz}$. The effect of a nonzero x is to move the d cones farther apart from each other, so that their radius in the direction that joins both d cones increases from $y/2$ (when $x=0$) to $\sqrt{y^2+x^2}/2$. If we assume that the main variation of the energy comes from the deformation in the intermediate region between both d cones, then, to lowest order in x, we have

$$\Delta E_b(x) = E_b - E_b^{(0)} \sim Yh^3 \epsilon^2 \frac{x^2}{y^2}. \tag{3}$$

But we note [11] that $\epsilon \sim \sqrt{z/R}$ and y have the same dependence in z, so that

$$\Delta E_b(x) \sim Yh^3 \left(\frac{x}{R}\right)^2 \tag{4}$$

is independent of z. As expected, the horizontal configuration $x=0$ is indeed minimizing the bending energy and therefore corresponds to the stable state of the system in the absence of torsion.

We consider now the influence of applied torsion. In Fig. 17 are presented typical measurements of the torque τ, in

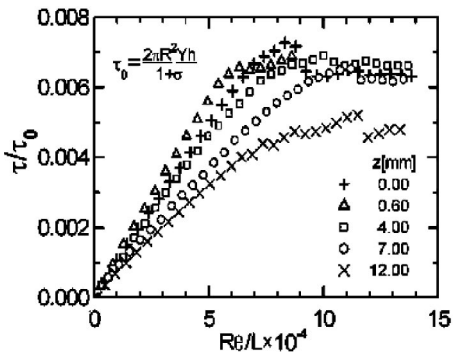

FIG. 17. Torque v/s torsion angle for different values of z. The thickness is 0.15 mm while $z_0 \approx 0.9$ mm.

units of $\tau_0 = 2\pi R^2 Yh/(1+\sigma)$, necessary to twist the cylinder up to an angle θ, for different values of z. The stored elastic energy due to the in-plane shear is directly seen on this graph as the area below the torque curves. For a given torsion angle θ, this energy first increases with z when $z < z_0$, but decreases when the finger is pushed further in—that is, when the d cones move away from each other. As expected, the movement of the d cones is associated with a release of energy which is due to a coupling between the deformation field around the d cones and the imposed shear field. The energy release, or coupling term, should be invariant under the simultaneous change $x \to -x$ and $\theta \to -\theta$, the lowest-order term satisfying this constraint being θx. We thus construct the gain of energy as $\Delta E_c(x) \sim -Y\eta(z,h)\ (x/R)\ (R\theta/L)$, where η is an unknown function.

The minimization of the energy, $\Delta E_c(x) + \Delta E_b(x)$, with respect to x thus gives the scaling law $x \sim \eta(z,h)h^{-3}\theta$. This relation gives the correct experimental dependence on θ and is compatible with the experimental relation (1) if $\eta(z,h) \sim h^2(z-z_0)$. This is the same dependence of the force acting on the tip (Fig. 6). As the stress field is expected to be proportional to this force, η can be interpreted as the amplitude of the stress field. The coupling energy becomes then

$$\Delta E_c(x) = -C_1 Y h^2 (z - z_0)\left(\frac{x}{R}\right)\left(\frac{R\theta}{L}\right), \tag{5}$$

where C_1 may depend on R, L (we did not scan these parameters).

Within this interpretation, the intermediate h^2 dependence of this energy shows that it is not a pure bending (h^3 dependence) or stretching (h dependence) energy, but rather a term involving a mixing of both. This is very much possible as we already noticed in Sec. IV B, where for $z \gtrsim 5h$ the lateral force scales roughly linearly with z and is proportional to h^2, thus also involving an h^2 scaling of the energies. However, the precise bending and stretching balance associated with the coupling field and singularity is not clearly evidenced here.

From the same balance one can derive the force F per thickness that drives the d cones to their new position. It reads

$$\frac{F}{h} \sim \sigma_0 h \frac{z - z_0}{R}, \tag{6}$$

where $\sigma_0 \sim YR\theta/L$ is the nominal shear stress. Expression (6) is valid only for $z > z_0$ and can be interpreted analogously to the Peach-Köhler force for an edge dislocation in a crystal. The line force is proportional to the product of the in-plane shear field and a quantity having the units of a length which can be interpreted as a "Burgers vector," having an amplitude proportional to the thickness of the sheet and, if $z \gg z_0$, to the square of the amplitude ϵ of the d cone.

VI. CONCLUSIONS

We have shown that a long cylindrical sheet clamped at its ends is an adequate experimental setup to study the behavior of d-cone-type singularities under various external forcing conditions. One important advantage of our experimental configuration is that boundary conditions are well defined.

An S structure consisting of two d cones linked by a stretched ridge is a characteristic feature at all stages of the scenario for large deformation of a thin cylindrical shell subject to pure axial torsion. We also observed the spontaneous formation of S structures and twisting on a closed cylindrical shell subject to inner decompression. Thus, twisting is a very efficient way for a cylinder to fold when its volume is reduced. Twisted folding along lines, reminiscent of the S structures in our crumpling experiment, has been described as a way to send large cylindrical structures for satellites, in a spatial ship occupying a minimal volume [15]. A good understanding of these S structures is necessary to describe the very large twisting of cylinders.

In addition, our experiment allows a quantitative study of an isolated S structure. In our case, a finger pushing the surface inwards creates a pair of d cones which evolve into an S structure when submitted to a sufficiently large shear stress. A collapse of all experimental points shows that the lateral size of the S structure is weakly dependent on torsion and is just given by geometry. In contrast, the experiment shows the existence of a critical value z_0 such that for $z > z_0$ the vertical size of the S structure is affected by external torsion. Experimental measurements show that this size is proportional to both the torsion angle θ and the variation of z, relative to the critical value z_0. It is also inversely proportional to the thickness of the sheet.

We interpret this evolution for increasing in-plane shear stress in terms of a gliding displacement undergone by the pair of d cones, in a manner analogous to the gliding motion of line dislocations in crystals through the Peach-Köhler force [14]. While in the latter case it is a dissipative effect that might induce a drift of the defect at constant velocity, in

our case such a force is stabilized by an increasing bending energy. It is proportional to the nominal shear stress σ_0 and grows with the amplitude ϵ of each d cone, above the threshold z_0. We believe that this rich but simple behavior provides a clean and precise landmark for a theory describing the interaction of d-cone singularities with an external stress field.

ACKNOWLEDGMENTS

The research of B.R. was supported by the FONDECYT Grant No. 3010001. We thank Arezki Boudaoud, Jean-Christophe Géminard, and Evgeny Podnos for valuable discussions. We also acknowledge Fernando Lund for a critical reading of the manuscript.

[1] N. Yamaki, *Elastic Stabilty Of Circular Cylindrical Shells* (North-Holland, Amsterdam, 1984).
[2] S. Timoshenko and J. Gere, *Theory of Elastic Stability* (McGraw-Hill, New York, 1961).
[3] T. A. Witten, Europhys. Lett. **23**, 51 (1993).
[4] A. E. Lobkovsky and T. A. Witten, Phys. Rev. E **55**, 1577 (1997).
[5] A. E. Lobkovsky, S. Gentges, H. Li, D. Morse, and T. A. Witten, Science **270**, 1482 (1995).
[6] M. Ben Amar and Y. Pomeau, Proc. R. Soc. London, Ser. A **453**, 729 (1997).
[7] S. Chaïeb, F. Melo, and J.-C. Géminard, Phys. Rev. Lett. **80**, 2354 (1998).
[8] E. Cerda and L. Mahadevan, Phys. Rev. Lett. **80**, 2358 (1998).
[9] K. Matan *et al.*, Phys. Rev. Lett. **88**, 076101 (2002).
[10] M. R. Falvo, G. J. Clary, R. M. Taylor II, V. Chi, F. P. Brooks, Jr., S. Washburn, and R. Superfine, Nature (London) **389**, 582 (1997).
[11] A. Boundaoud, P. Patricio, Y. Couder, and M. Ben Amar, Nature (London) **407**, 718 (2000).
[12] G. J. Lord, A. R. Champneys, and G. W. Hunt, in *IUTAM Symposium on New Applications of Nonlinear and Chaotic Dynamics in Mechanics*, edited by Francis C. Moon (Kluwer, Dordrecht, 1997),
[13] L. Landau and E. Lifchitz, *Théorie de l'Élasticité*, 2nd ed. (Mir, Moscow 1990).
[14] M. Peach and J. S. Koehler, Phys. Rev. **80**, 436 (1950).
[15] S. D. Guest and S. Pellegrino, J. Appl. Mech. **61**, 773 (1994).